Study of Radiation Effects on Bipolar Transistors

A. Colder[1], N. Croitoru[2,3], P. D'Angelo[2], M. De Marchi[2,4], G. Fallica[4], S. Leonardi[4], M. Levalois[1], S. Marcolongo[2], P. Marie[1], R. Modica[4], P.G. Rancoita[2] and A. Seidman*[2,3].

[1] Lermat, Caen, France

[2] INFN – Istituto Nazionale di Fisica Nucleare, sezione di Milano, Milan, Italy.

[3] Department of Physical Electronics, Tel-Aviv University, Ramat Aviv, Israel

[4] STMicroelectronics, Catania, Italy

Abstract

In this paper it was shown that the irradiation with neutrons and carbon ions lead to gain degradation in bipolar transistors due to generation of defects. The density of these generated defects is independent on type of irradiation (neutrons or carbon ions). Thus, it is possible to evaluate $\Delta(1/\beta)$, once the expected Frenkel pairs density is known.

The dependence of the damage constant on collector current, is a power law function, with the exception of the lateral pnp transistors, that shows a higher sensitivity to radiation and a different behaviour.

Neutrons give a smaller density of Frenkel pairs (CF) than the two sorts of carbon ions of high energy(CHE) and medium energy (CME). It was found that CME cause a higher concentration of CF. The calculated ratio $R = CF/\Phi$, where CF is the Frenkel pair density and Φ fluence does not depend on Φ, for a given type of radiation. However, it depends on incoming particle type. Its smallest calculated value was obtained for neutrons ($R= 6.1\text{x}10$), which increases to $1.25\text{x}10^3$ for CHE and to $1.1\text{x}10^4$ for CME.

1 INTRODUCTION

In recent years, intensive investigation of radiation hardness of BJT and MOS devices, integrated in BiCMOS technology was done [1-6], in order to analyse the performance changes of the individual devices and to find better design strategies.

Measurements of the radiation effects on the npn and pnp transistors (HF2CMOS process) are presented. The base current (I_b), the collector current (I_c), and the forward gain (β_F) as a function of polarisation, before and after irradiation with neutrons, and carbon ions, were measured and analysed. A correlation between the variations of β_F and the concentration of defects produced in the silicon bulk by irradiation, were found.

2 DEVICES AND METHODS

The investigated devices were manufactured by ST-Microelectronics, using an industrial standard high-speed technology, called HF2CMOS. Devices were irradiated by neutrons, carbon ions, or by both of them.

The neutron irradiation was performed at the Triga reactor RC:1 of the National Organisation of Alternative Energy (ENEA) at Casaccia, Rome. The flux of the reactor, in the energy range of 24.8keV - 10MeV, was 6.474×10^{11}n/cm^{2}s, at the reactor power of 1MW. The obtained fluences were in the range of 1.0×10^{13}n/cm^2 - 1.0×10^{15}n/cm^2 (see Table 1).

Neutron fluences [n/cm^2]	Carbon fluences [C/cm^2] HE	Carbon fluences [C/cm^2] ME
1.2×10^{13}	5.2×10^{10}	1.0×10^{11}
1.2×10^{14}	1.0×10^{11}	5.0×10^{11}
6.0×10^{14}	5.1×10^{11}	1.0×10^{12}
1.2×10^{15}	1.0×10^{12}	5.0×10^{12}
	5.0×10^{12}	1.0×10^{13}
	1.0×10^{13}	1.0×10^{14}

Table 1. Fluences used in the irradiation tests.

The carbon ions were made available at the Grand Accelerateur National d'Ions Lourds (GANIL), at two different energies: a. ^{12}C accelerated at 95 MeV/a (High Energy, HE), and b. ^{13}C ions at energy of 11.1 MeV/a (Medium Energy, ME).

Both npn and pnp devices were characterised, using a modular DC source/monitor (Hewlett-Packard HP4142B), controlled by a work station HP9000/C160. The forward voltage applied to the emitter-base junction (V_{BE}), was in the range 0.2V-1.2V, which allows to measure the value of β_F for $10^{-12}<Ic<5x10^{-3}A$, with the base and collector grounded. The measurement was done using the same setup before and after irradiation. Due to the intrinsic technological spread of the β_F values, all the samples were measured before irradiation, in order to correctly evaluate the variations for each sample, due to irradiation. For each fluence, two of the three transistors were irradiated. All the measurements were done at room temperature (T~25°C). The samples, irradiated by medium energy carbon, were measured in a climatic chamber, at a constant temperature value of 24°C.

3 DEFECTS CALCULATION

The gain degradation of bipolar junction transistors under neutron irradiation can be considered as a function of the interstitial-vacancy Frenkel pairs [7-9]. junction transistors the gain degradation can A way of normalising the damage, caused from different spectra to the neutron energy of 1MeV and it given in ASTM standards [8]. In a neutron collision in silicon, a primary displacement can be caused. If the incident energy is sufficiently high, the displaecement Si ion can generate secondary displacements. Thus, defects are produced in clusters. In literature [8], the energy dependent neutron displacement cross-section cross-section in silicon, given in kerma, Furthermore, it is possible to obtain the energy loss in the lattice, El, due to the creation of defects, as:

$$(1) \qquad El = \int_{E\min}^{E\max} N\phi(E)k(E)dE$$

where ϕ is the fluence, N the atomic density, and k the cross section expressed in kerma, E is the neutron kinetic energy.

It is also possible to calculate the density of Frenkel pairs, by dividing k(E) to $2E_d$, where E_d is the displacement energy. In the present paper, E_d is about 25eV and, thus, the displacement cross-section is:

$$\sigma_d(E) = \frac{k(E)}{2E_d} \tag{2}$$

Then the density of defects, generated in the lattice can be calculated:

$$N_d = \int N\phi(E)\sigma_d(E)dE\ . \tag{3}$$

Ion irradiation effects on silicon were calculated, using the Monte Carlo simulation program Trim [10]. Since ions range varies with energy, it is important to evaluate the depth at which the device is realized inside the substrate. The samples are mounted inside a package with removable upper lid. Therefore, it is also possible to irradiate the samples with ions at low energy, namely large values of collision energy losses.

The range of carbon ions at medium energy (11.1MeV/a) is between 300 and 350µm. Since during the slowing down of the ions, the production of density of Frenkel pairs varies, we have investigated the first 10µm thick layer, where the active region is located. Inside this layer, the simulations showed a uniform defect-production. For carbon ions at high energy, the Frenkel pairs production is uniform for more than 300µm, in depth.

In Table 2, the calculated values for each kind of irradiation are presented. In Table 3, the data are collected and ordered with respect to the Frenkel pairs.

Radiation	Frenkel pairs [cm^{-3}]
n [cm^{-2}]	60.9
CHE [cm^{-2}]	1234
CME [cm^{-2}]	10700

Table 2: Frenkel pairs concentration per incident particle for each kind of irradiation, where n is neutrons, CHE-High Energy carbon ions, and CME-Medium Energy carbon ions.

Radiation	Dose/Fluence [cm^{-2}]	Frenkel pairs [cm^{-3}]
CHE	5.2×10^{10}	6.4×10^{13}
CHE	1.0×10^{11}	1.3×10^{14}
CHE	5.1×10^{11}	6.3×10^{14}
N	1.2×10^{13}	7.3×10^{14}
CME	1.0×10^{11}	1.1×10^{15}
CHE	1.0×10^{12}	1.3×10^{15}
CME	5.0×10^{11}	5.4×10^{15}
CHE	5.0×10^{12}	6.2×10^{15}
N	1.2×10^{14}	7.3×10^{15}
CME	1.0×10^{12}	1.1×10^{16}
CHE	1.0×10^{13}	1.2×10^{16}
N	6.0×10^{14}	3.7×10^{16}
CME	5.0×10^{12}	5.4×10^{16}
N	1.2×10^{15}	7.3×10^{16}
CME	1.0×10^{13}	1.1×10^{17}
CME	1.0×10^{14}	1.1×10^{18}

Table 3: Collection of all available data

4 RESULTS

4.1 Data analysis

The collected gains before and after irradiation were performed using the collector current Ic as a parameter.

All the data at fixed I_C, show an almost linear dependence of a $\Delta(1/\beta)$ on the Frenkel pairs density.

In Figs.1 and 2, the gain variation $\Delta(1/\beta)$ for 1µA and 1mA collector current are shown for 5x5 npn transistors (emitter region 5µmx5µm), minimum area in this technology.

A linear fit was used, see continuous line overposed in Figs.1 and 2, to find the slope that corresponds to:

$$\text{(4)} \quad \Delta\left(\frac{1}{\beta}\right) = k \cdot CF$$

where CF is the Frenkel pairs density.

In [7, 9] the same law is presented, for a given particle or spectrum, with a dependence on the fluence. The damage constant k, is known to be inversely proportional to the cut-off frequency. The lateral pnp have a lower cut-off frequency (20MHz versus 2-6 GHz of vertical pnp and npn.

If the damage is constant (the slope of the fit) for plotting with the collector current, it is possible to find a regular behaviour of the values, that follows a power law (Fig. 3).

The 50x50 npn transistor (emitter region 50µmx50µm) were irradiated with ions only. They still exhibit linearity for a given collector current (Fig. 4) and the regular behaviour of the slope (Fig. 5). The damage effects appear to be higher in these devices than on the ones with smaller area.

Vertical pnp transistors were irradiated only with carbon ions at medium energy, but they still exhibited the same behaviour (Figs. 6 and 7).

Lateral pnp were irradiated with neutrons and ions. As expected, because of their lower cut-off frequency, they showed greater damage effects, still observing the linearity with the Frenkel pairs (Fig. 8), but the slope dependence with the collector current was different and not regular, descending and then increasing (Fig. 9).

5 CONCLUSIONS

The experimental data show that the gain degradation in bipolar transistors depends on the defects density generated in the devices and is independent on the type of irradiation. Thus, it is possible to evaluate $\Delta(1/\beta)$, once the expected Frenkel pairs density is known.

The dependence of the damage constant with collector current, was a power law function, with the exception of the lateral pnp transistors, that shows a higher sensitivity to radiation and a different behaviour.

Neutrons give a smaller density of Frenkel pairs (CF) than both sorts of carbon ions (CHE and CME). The smaller energy carbon ions (CME) cause a higher concentration of CF, shown in Table 3. The calculated ratio R = CF/Φ, where CF is the Frenkel pair density and Φ fluence (taken from Table 3), does not depend on Φ, for a given type of radiation. However, it depends on incoming particle type. Its smallest calculated value was obtained for neutrons (R= 6.1x10), which increases to 1.25×10^3 for CHE and for CME to 1.1×10^4.

REFERENCES

[1] A.Baschirotto et al., Nucl. Instr. and Meth. A 362 (1995) 466.

[2] A.Baschirotto et al., Nucl. Instr. and Meth. B 114 (1996) 327.

[3] A.Baschirotto et al., Nucl. Instr. and Meth. B 122 (1997) 73.

[4] S.Caruso et al., “RHBIP1 Technology Evaluation to Total Dose, Low Dose Rate and Neutrons, for LHC Experiments and Space Applications”, presented at RADECS-97.

[5] D.M.Fleetwood et al., IEEE Trans. Nucl. Sci. NS-41(6) (1994) 1871.

[6] A.H.Johnston et al., IEEE Trans. Nucl. Sci. NS-41(6) (1994) 2427.

[7] G.C.Messenger and M.S.Ash, “The Effects of Radiation on Electronic Systems”, Van Nostrand Reinhold Company, New York, 1986.

[8] ASTM E722-85

[9] A.Holmes-Siedle, L.Adams, Handbook of Radiation Effects, Oxford University Press, 1993

[10] J.F.Ziegler, J.P.Biersack, U.Littmark, “The Stopping and Range of Ions in Solids”, Pergamon Press, New York, 1985.

[11] S.Leonardi, Attività Rad-hard, report fase irraggiamento 1 - R.T.N. 23_99/LNS ST Microelectronics, 1999.

FIGURE CAPTIONS

Fig. 1. Linear dependence of $\Delta(1/\beta)$ on Frenkel Pairs density, npn 5x5, Collector current 1μA. The linearity of the fit is observed and does not depend on the particle type or energy.

Fig. 2. Linear dependence of $\Delta(1/\beta)$ on the Frenkel Pairs density, npn 5x5, Collector current 1mA. The linearity of the fit is observed and does not depend on the particle type or energy.

Fig. 3. npn 5x5. Collection of the damage constant k (the slope of the fit). The slope depends on the collector current and follows a power law.

Fig. 4. Linear dependence of $\Delta(1/\beta)$ on Frenkel Pairs density, npn 50x50, Collector current 1μA. The linearity of the fit is observed as on the devices with smaller area.

Fig. 5. npn 50x50. Collection of the damage constant k (the slope of the fit). The slope depends on the collector current and follows a power law.

Fig. 6. Vertical pnp. Linear dependence of $\Delta(1/\beta)$ with the Frenkel Pairs density for a collector current of 1mA. The behaviour is the same as the one seen on npn devices.

Fig. 7. Vertical pnp. Collection of the damage constant k (the slope of the fit). The slope depends on the collector current and follows a power law, as on the npn devices.

Fig. 8. Lateral pnp. Linear dependence of $\Delta(1/\beta)$ on Frenkel Pairs density for a collector current of 1μA. The damage is higher in these devices.

Fig. 9. Lateral pnp. Collection of the damage constant k (the slope of the fit). The slope depends on the collector current, like for the other devices, but does not follow the power law seen in the other cases.

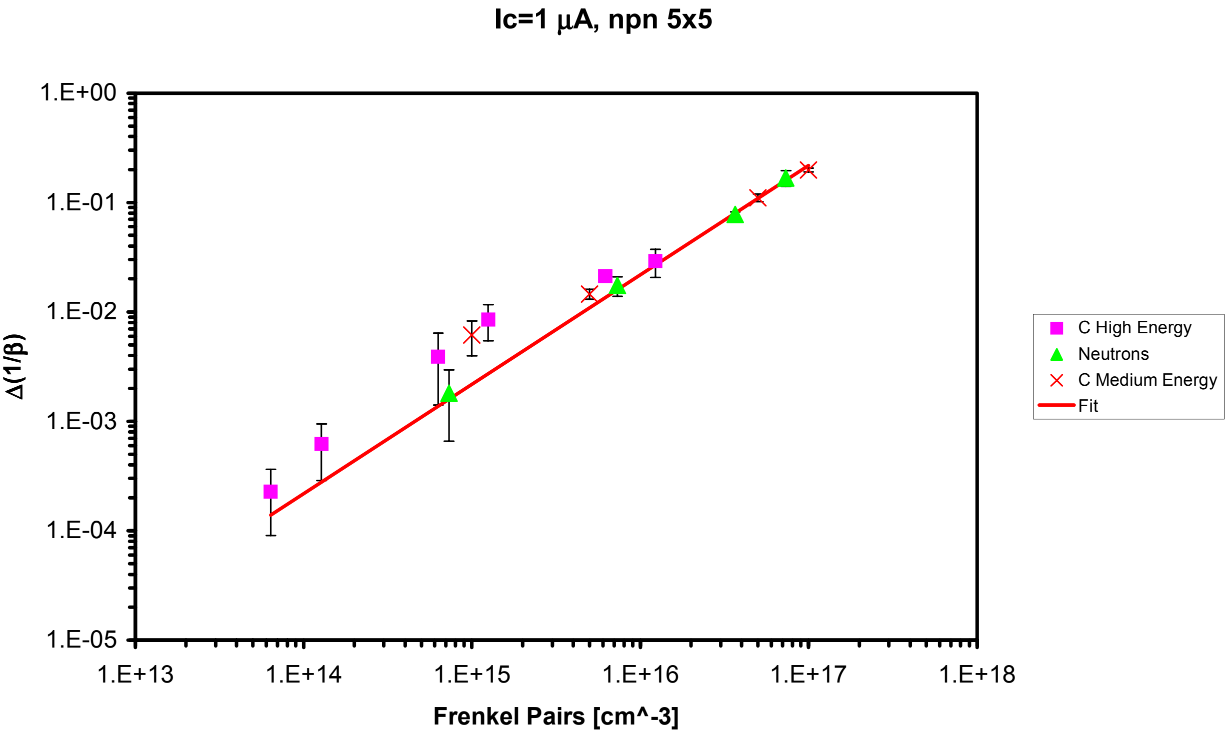
Ic=1 µA, npn 5x5
Δ(1/β)
1.E+00
1.E-01
1.E-02
1.E-03
1.E-04
1.E-05
1.E+13
1.E+14
1.E+15
1.E+16
1.E+17
1.E+18
Frenkel Pairs [cm^-3]
C High Energy
Neutrons
C Medium Energy
Fit

Fig. 1

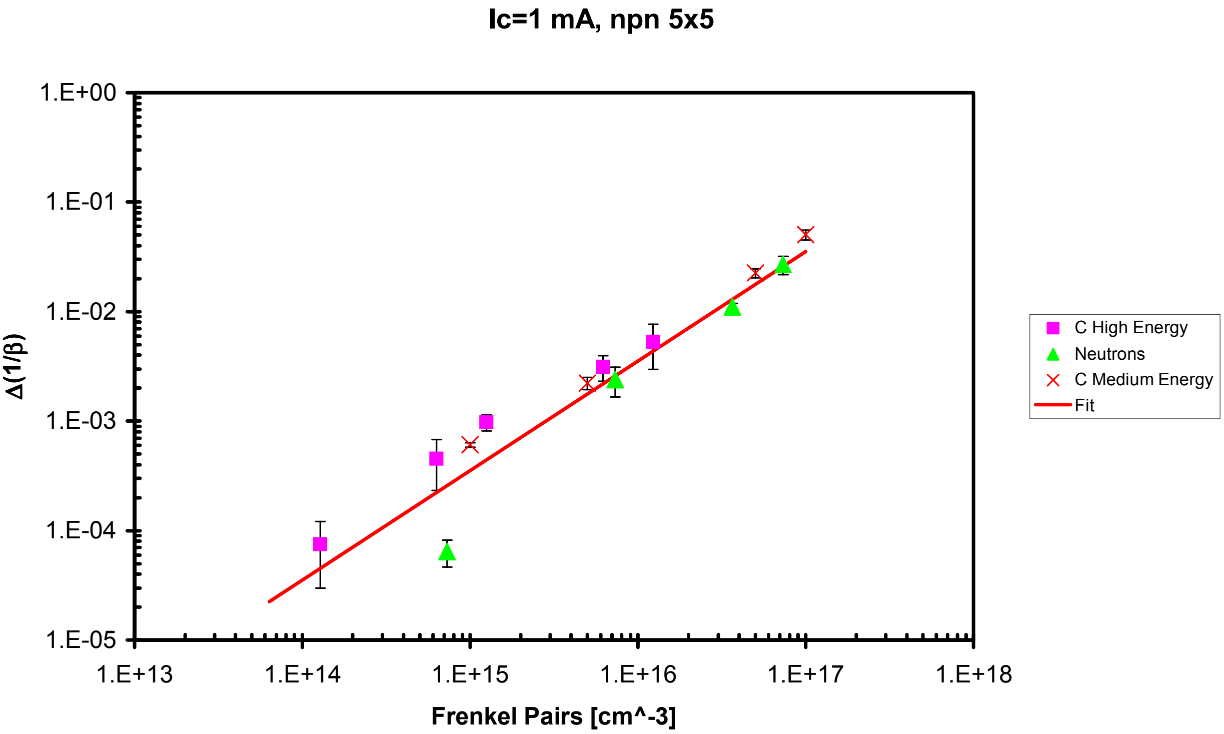
Ic=1 mA, npn 5x5
Δ(1/β)
1.E+00
1.E-01
1.E-02
1.E-03
1.E-04
1.E-05
1.E+13
1.E+14
1.E+15
1.E+16
1.E+17
1.E+18
Frenkel Pairs [cm^-3]
C High Energy
Neutrons
C Medium Energy
Fit

Fig. 2

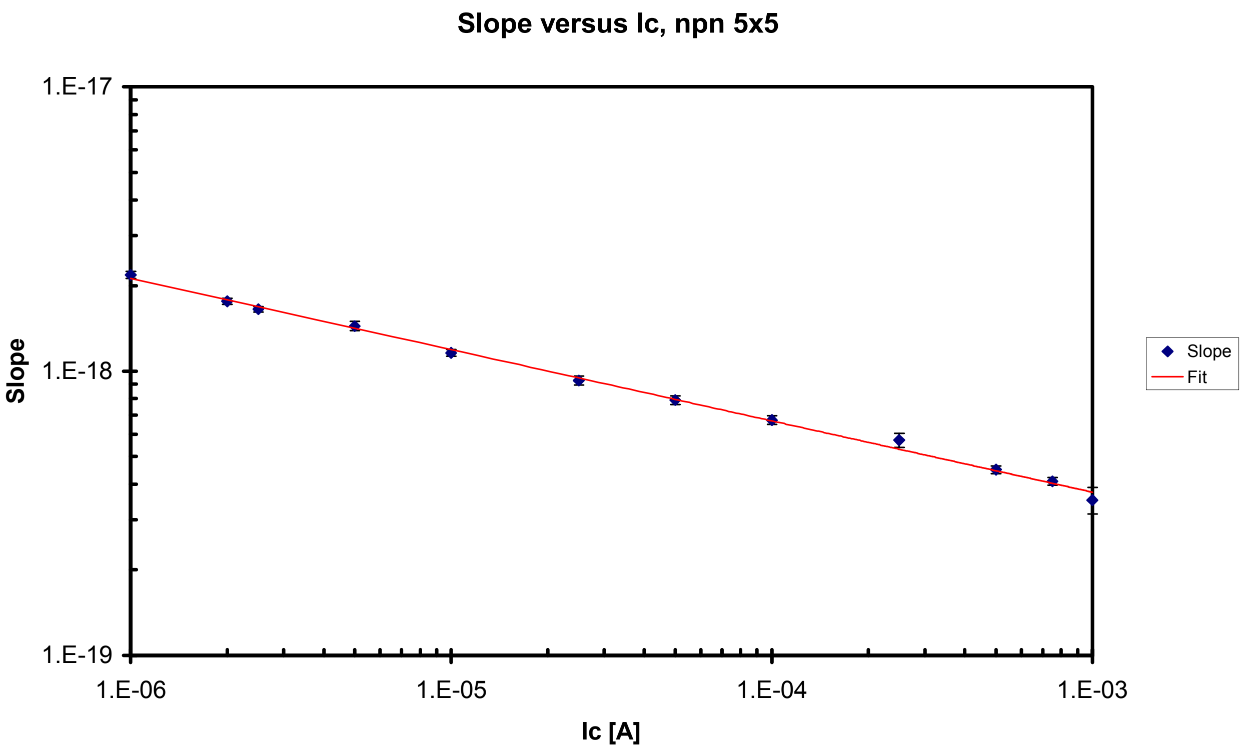
Slope versus Ic, npn 5x5
1.E-17
1.E-18
1.E-19
Slope
1.E-06
1.E-05
1.E-04
1.E-03
Ic [A]
◆ Slope
Fit

Fig. 3

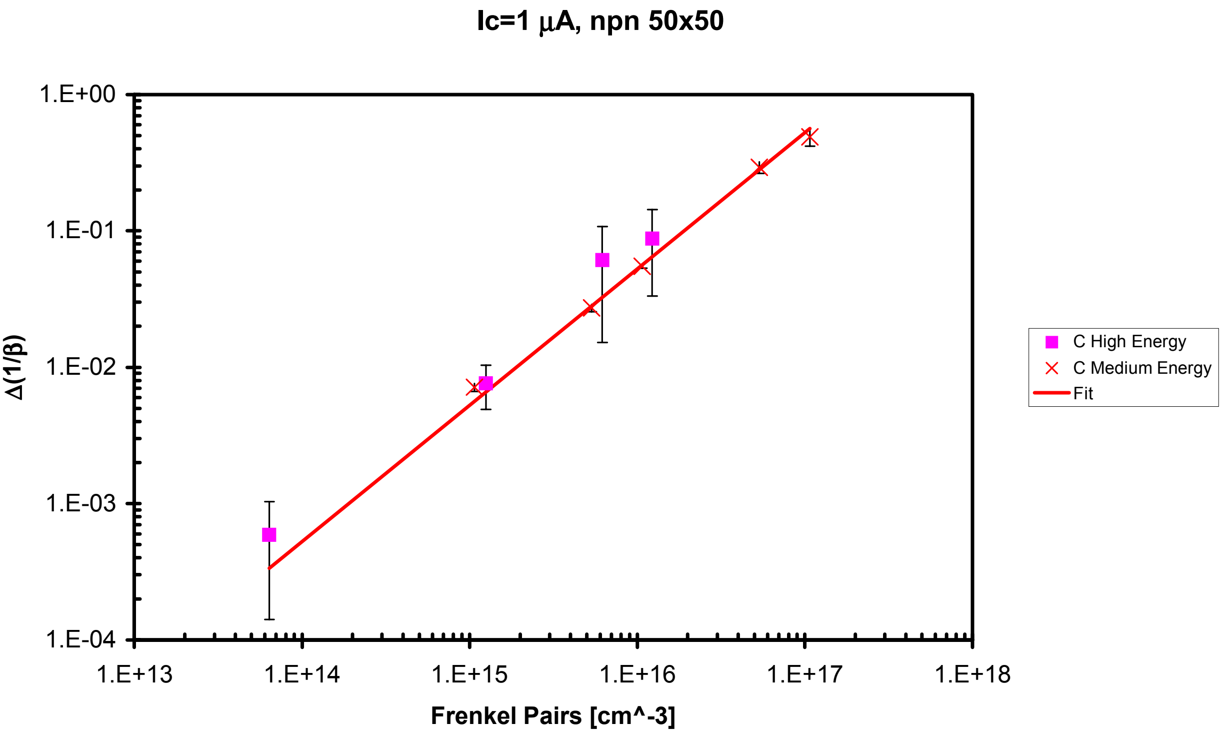
Ic=1 μA, npn 50x50
1.E+00
1.E-01
1.E-02
1.E-03
1.E-04
Δ(1/β)
1.E+13
1.E+14
1.E+15
1.E+16
1.E+17
1.E+18
Frenkel Pairs [cm^-3]
C High Energy
C Medium Energy
Fit

Fig. 4

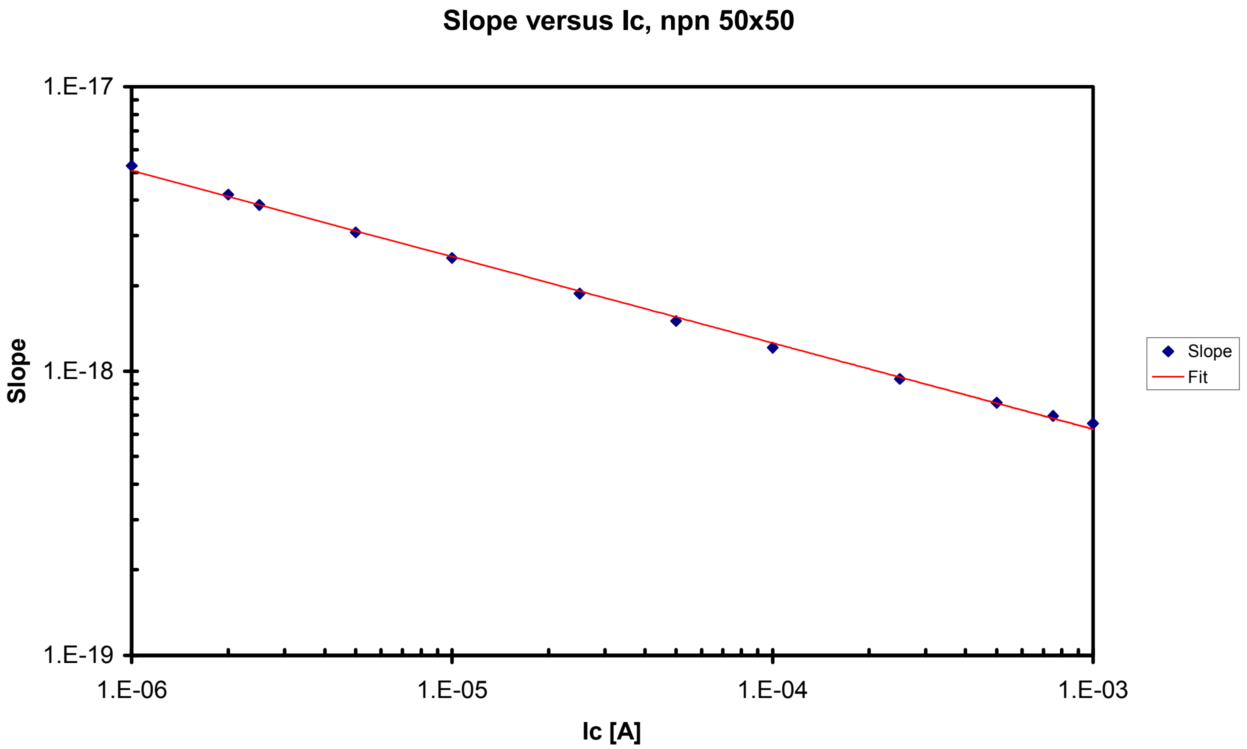
Slope versus Ic, npn 50x50
1.E-17
1.E-18
1.E-19
Slope
1.E-06
1.E-05
1.E-04
1.E-03
Ic [A]
Slope
Fit

Fig. 5

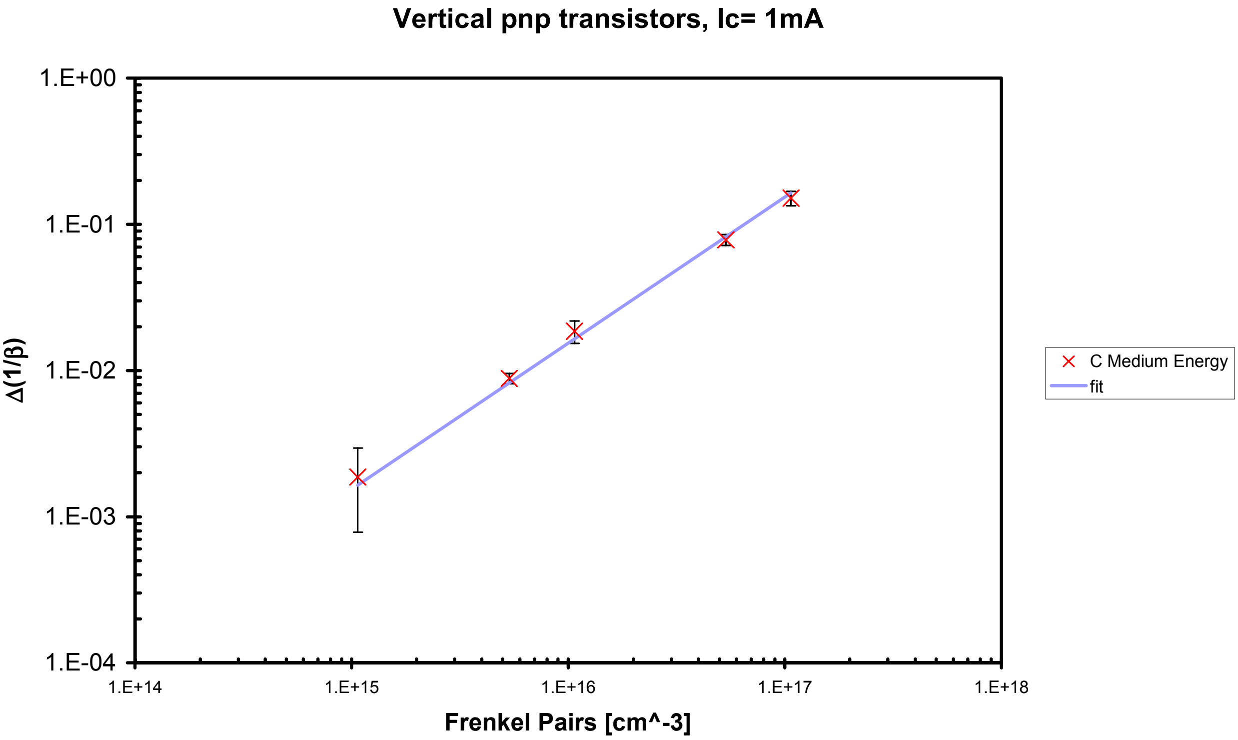
Vertical pnp transistors, Ic= 1mA
1.E+00
1.E-01
1.E-02
1.E-03
1.E-04
Δ(1/β)
1.E+14
1.E+15
1.E+16
1.E+17
1.E+18
Frenkel Pairs [cm^-3]
C Medium Energy
fit

Fig. 6

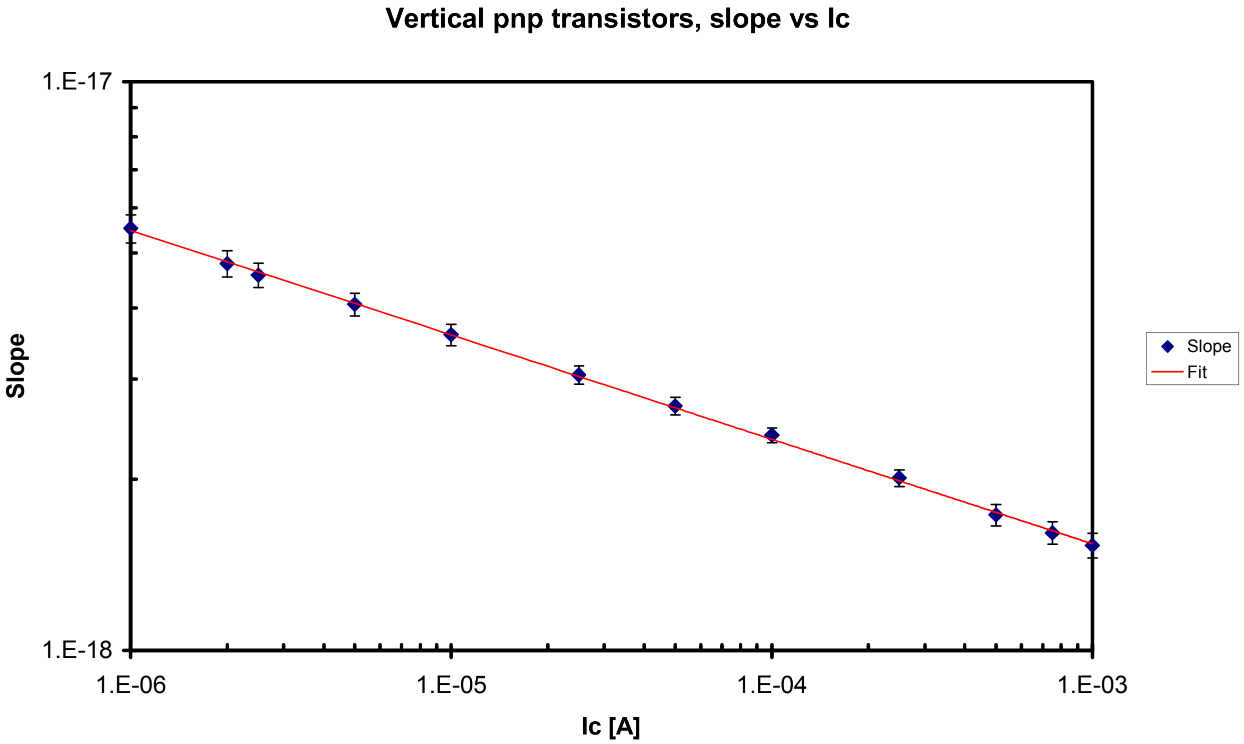
Vertical pnp transistors, slope vs Ic
1.E-17
1.E-18
Slope
1.E-06
1.E-05
1.E-04
1.E-03
Ic [A]
◆ Slope
Fit

Fig. 7

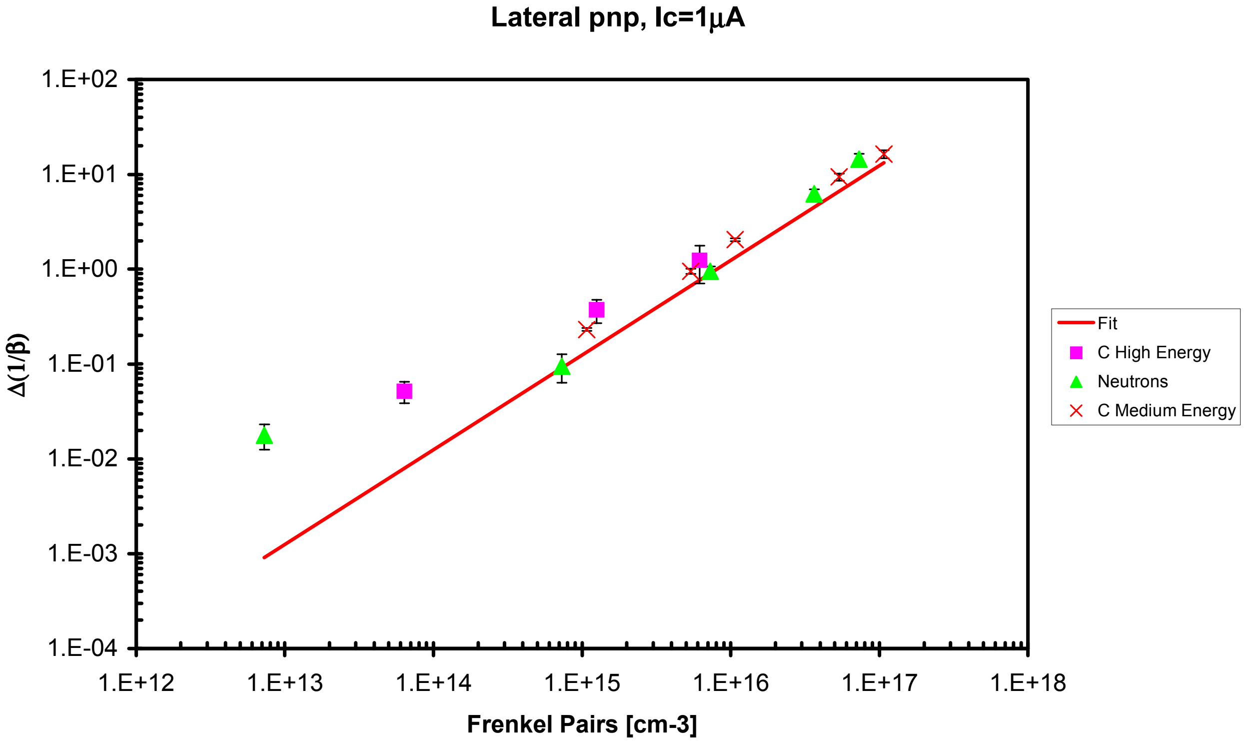
Lateral pnp, Ic=1μA
1.E+02
1.E+01
1.E+00
1.E-01
1.E-02
1.E-03
1.E-04
Δ(1/β)
1.E+12
1.E+13
1.E+14
1.E+15
1.E+16
1.E+17
1.E+18
Frenkel Pairs [cm-3]
Fit
C High Energy
Neutrons
C Medium Energy

Fig. 8

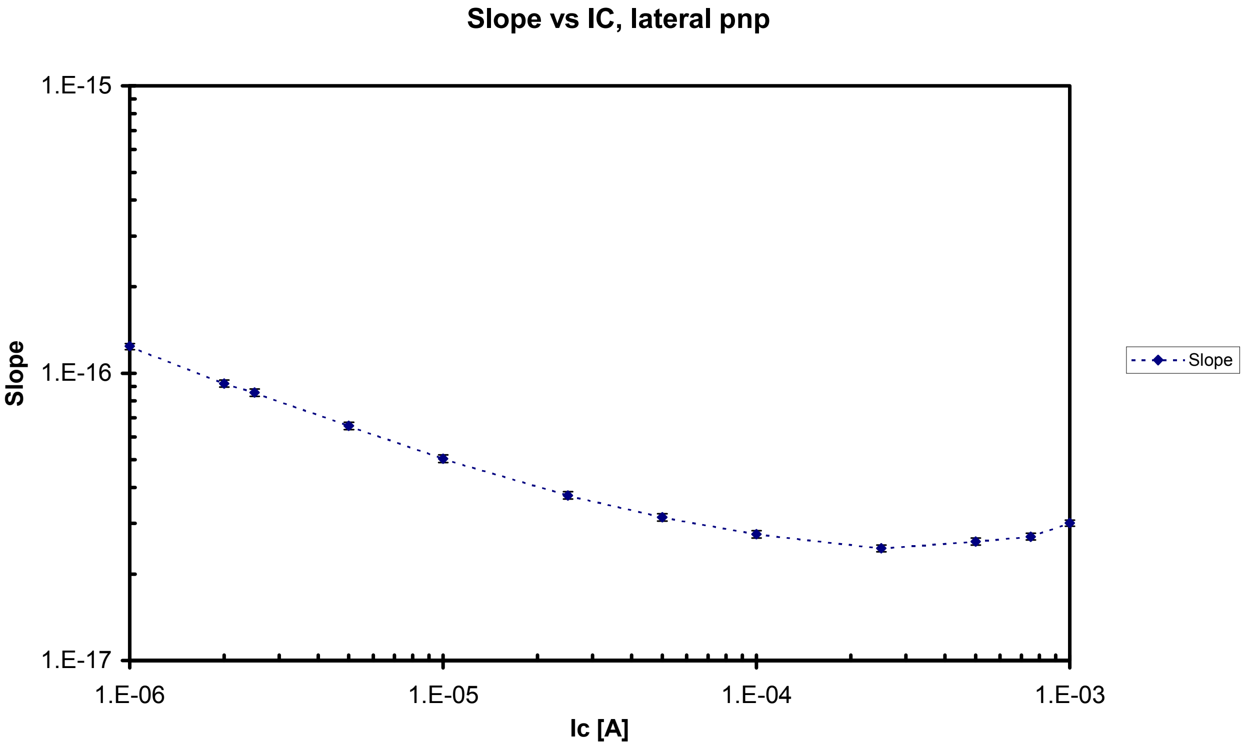
Slope vs IC, lateral pnp
1.E-15
1.E-16
1.E-17
Slope
1.E-06
1.E-05
1.E-04
1.E-03
Ic [A]
Slope

Fig. 9